

Design and Synthesis of N-4-(substituted benzylidene)-N-2-(4-chloropyrimidin-2-yl)-6, 7-dimethoxyquinazoline-2, 4-diamines as Anticancer Agents

Shweta A. More, Nikhil Sakle and Santosh N. Mokale*

Dr. Rafiq Zakaria Campus, Y. B. Chavan College of Pharmacy, Aurangabad, 431001, Maharashtra, India

*Corresponding author (e-mail: santoshmokale@rediffmail.com)

A novel series of N-4-(substituted benzylidene)-N-2-(4-chloropyrimidine-2-yl)-6,7-dimethoxyquinazoline-2,4-diamine compounds were designed, synthesized and evaluated for their anti-cancer properties. The structures of the target derivatives were elucidated using spectral techniques like ^1H NMR, ^{13}C NMR and mass spectroscopy. All the designed compounds were tested for their probable anti-cancer activity on human colon-rectal cell lines (HT-29 and COLO-205), followed by cell-cycle analysis, apoptosis assays, and enzyme inhibitory assays. VEGFR-2 kinase inhibitory assays and cell cycle analyses were performed to validate the target selectivity of the designed compounds. Among the synthesized derivatives, **SM-8** ($\text{GI}_{50} = 10.64 \mu\text{M}$) showed good inhibition activity against HT-29 cell lines. Cellular mechanism studies confirmed that compound SM-8 could induce apoptosis in HT-29 cells in G1 phase, which was concentration-dependent. In order to evaluate the specific interaction with tyrosine kinase, designed scaffolds were subjected to docking, *in-silico* physicochemical properties and ADME prediction studies. MM/GBSA was performed to calculate the ligand binding free energies.

Key words: Quinazoline; *in-vitro* activity; molecular Docking; *in-silico* ADME study

Received: April 2022; Accepted: September 2022

Receptor Tyrosine Kinases (RTKs) play a vital role in various cellular processes and signal transduction pathways. In the current era RTKs have been found to have divergent roles in different chemo-therapeutic medications. RTKs play an important role in phosphorylating the tyrosine amino acid in several proteins with the help of ATP (γ -phosphoryl group donor). Phosphorylation ultimately leads to activation of a signalling pathway at the cellular level which includes crucial processes for differentiation, proliferation, migration, and antiapoptotic pathways. The c-mesenchymal epithelial transition factor (c-MET) is a widely over-expressed RTK in human tumours and a receptor for hepatocyte growth factor (HGF). HGF binding to c-Met causes phosphorylation of tyrosine residues on c-Met, which activates the downstream signalling pathway involved in cell proliferation, invasion, metastasis, and angiogenesis in a variety of cancers. c-Met activation has been linked to poor clinical outcomes in a variety of human solid tumours and haematological cancers [1,2]. Additionally, c-Met overactivation leads to therapeutic resistance. As a result of resistance, inhibiting c-Met activity could be a promising treatment option for malignancies. Small molecule inhibitors of c-Met can be divided into several types based on their binding mechanisms. Multikinase inhibitors, for example, are a common form of c-Met inhibitor that also inhibits VEGFR and other Homologous kinases.

Endothelial cells contain a tyrosine kinase receptor known as vascular endothelial growth factor receptor 2 (VEGFR-2, also known as KDR). When VEGF binds to VEGFR, it causes a conformational shift in the receptor, which is followed by dimerization and phosphorylation of tyrosine residues [3]. VEGFR-2-mediated VEGF signalling has been found to play a key role in tumour angio-genesis regulation. VEGF expression is increased in a variety of human cancers, and high levels of VEGF are linked to a poor prognosis and clinical stage in patients with solid tumours. As a result, VEGF/VEGFR-2 signalling represents a promising therapeutic target in cancer treatment. The synergistic collaboration of c-Met and VEGFR-2 has been shown to promote angiogenesis in the development and progression of several human malignancies [4, 5, 11]. As a result, compounds that inhibit both c Met and VEGFR-2 at the same time may be preferable to c Met- or VEGFR-2-specific inhibitors because they can disrupt numerous signalling pathways involved in tumour proliferation, metastasis, and angiogenesis. Several kinase inhibitors, such as cabozantinib and foretinib, have been shown to suppress both c-Met and VEGFR-2 kinases at the same time. Consequently, we began developing dual c-Met and VEGFR-2 TKIs with substantial anti-tumour effectiveness using the quinazoline nucleus, which is widely used in drug development, particularly in RTK inhibitors [6].

Quinazoline and its derivatives have been considered an important class of chemotherapeutic agents [7, 8] Fused pyrimidine has been demonstrated to have remarkable anticancer potential [9,10,11]. Thus, taking into consideration the anticancer effects of heterocyclic compounds, we have designed the scaffold which includes: A central aromatic or heterocyclic ring (quinazoline), a linker as the aliphatic chain containing a hydrogen donor and acceptor, Ring A as the aromatic or heterocyclic ring with a hydrogen donor and acceptor group (pyrimidine) and Ring B, the aromatic or heterocyclic ring with a hydrophobic group (substituted aldehydes) as shown in **Figure 1**. The docking study was carried out with nine important receptors of cancers in order to determine their interactions with the designed scaffolds. In addition, *in-silico* physicochemical properties and ADME properties were also predicted.

EXPERIMENTAL SECTION

1. Synthesis and Characterization

All reagents were purchased from commercial sources and used without further purification. The traditional approach was used to carry out the synthesis. The SRS Optimelt melting point equipment was used to determine melting points. Nuclear magnetic resonance (¹H-NMR and ¹³C-NMR) spectra were obtained with a ECZR series 600 MHZ NMR (JEOL, Japan) at IIT SAIF, Mumbai. S stands for singlet; d for doublet; t for triplet; q for quartet; dd for doublet of doublet; ddd for doublet of doublets; br for wide singlet; m for multiplet. At IIT SAIF in Mumbai, mass spectra (MS) were recorded on an Element XR. TLC sheets coated with UV fluorescent silica gel Merck 60 F254 plates were used to monitor the reaction, which was observed under UV light and utilized several solvents.

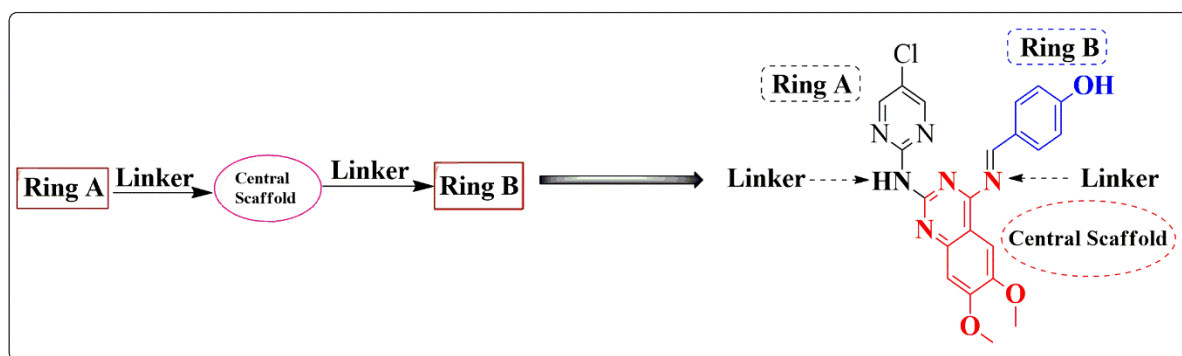
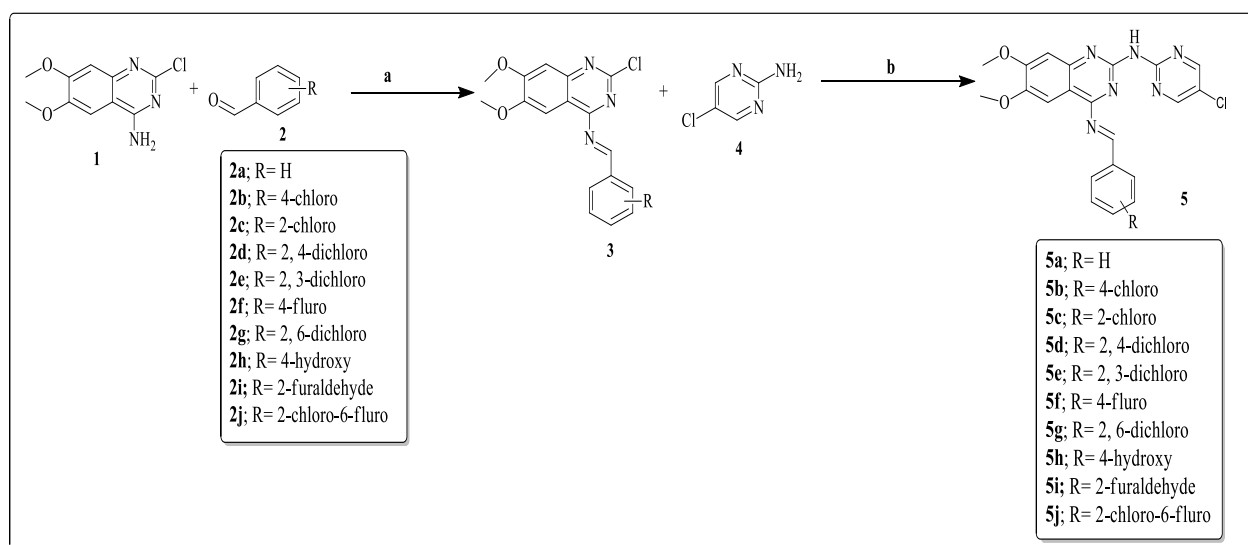


Figure 1. Designing strategy and scaffold of novel Chloropyrimidine Quinazoline anti-cancer inhibitors.



Scheme 1. Reagents and conditions: (1) 2-Chloro-6, 7-dimethoxyquinazolin-4-amine, (2) Substituted Benzaldehyde, (a) glacial acetic acid, EtOH, reflux; (3) Substituted benzylidene-2-chloro-6, 7-dimethoxyquinazolin-4-amine, (4) 2-amino-5-chloropyrimidine, (b) K₂CO₃, DMF, reflux and (5) Substituted benzylidene-(5-chloropyrimidin-2-yl)-6, 7-dimethoxyquinazolin-2, 4-diamine

1.1. General Procedure for Synthesis of Substituted Benzylidene-2-chloro-6,7-dimethoxyquinazolin-4-amine

2-chloro-6,7-dimethoxyquinazolin-4-amine and a substituted aldehyde (1:1) were dissolved in ethanol (10 ml) followed by the addition of glacial acetic acid (2 drops). The reaction mixture was allowed to reflux for 24 hours. After completion of the reaction as indicated by TLC, the reaction mixture was diluted with 100 ml of ice-cold water. The intermediate was filtered and the obtained product was recrystallized using ethanol as a solvent to obtain fine crystals [12].

1.2. General Procedure for Synthesis of Substituted Benzylidene-(5-chloropyrimidin-2-yl)-6,7-dimethoxyquinazolin-2,4-diamine

Once the fine crystals were obtained, the intermediate was reacted with 2-amino-5-chloropyrimidine (1:1) using DMF and anhydrous potassium carbonate (3 equivalents) [13]. After completion of the reaction, the mixture was diluted with 100 ml of ice-cold water. The final product was filtered and recrystallized using ethanol as a solvent to obtain fine crystals (Scheme 1).

N4-benzylidene-N2-(4-chloropyrimidin-2-yl)-6,7-dimethoxyquinazolin-2,4-diamine(SM-1): White crystals, (Yield: 87 %), (M.P.: 260 °C); ¹H NMR (400 MHz, CDCl₃): δ 3.86 (3H, s), 3.95 (3H, s), 6.74 (1H, d, *J* = 5.7 Hz), 7.13 (1H, d, *J* = 0.4 Hz), 7.37 (1H, tdd, *J* = 7.4, 1.7, 1.5 Hz), 7.45 (2H, dddd, *J* = 7.8, 7.4, 1.4, 0.4 Hz), 7.59 (1H, d, *J* = 0.4 Hz), 7.82 (1H, d, *J* = 5.7 Hz), 8.34 (2H, dtd, *J* = 7.8, 1.6, 0.4 Hz), 9.24 (1H, s). δ (ppm) ¹³C (400 MHz, CDCl₃) 128.92353, 103.05, 128.7361, 128.7361, 162.19412, 151.63397, 120.3, 56.15704, 162.60001, 106.39285, 153.92217, 149.17067, 148.76202, 147.26062, 56.15704, 135.7, 162.19412, 150.1025, 128.8716, 128.8716, 113.86571, 420.85. Anal. Calc. for C₂₁H₁₇ClN₆O₂: C, 59.93; H, 4.07; N, 19.97; O, 7.60; Cl, 8.42. Found: C, 59.90; H, 4.03; N, 19.92; O, 7.56; Cl, 8.40. HR-MS (ESI) *m/z*: Calculated for [M+H] ⁺420.857.

N4-(2-chlorobenzylidene)-N2-(4-chloropyrimidin-2-yl)-6,7-dimethoxyquinazolin-2,4-diamine (SM-2): White crystals, (Yield: 84 %), (M.P.: 240 °C); ¹H NMR (400 MHz, CDCl₃): δ 3.88 (3H, s), 3.95 (3H, s), 6.74 (1H, d, *J* = 5.7 Hz), 7.11 (1H, d, *J* = 0.4 Hz), 7.40-7.50 (2H, 7.46 (ddd, *J* = 7.6, 7.4, 1.1 Hz), 7.45 (ddd, *J* = 7.9, 7.4, 1.5 Hz)), 7.56 (1H, d, *J* = 0.4 Hz), 7.72 (1H, ddd, *J* = 7.9, 1.1, 0.5 Hz), 7.82 (1H, d, *J* = 5.7 Hz), 7.96 (1H, ddd, *J* = 7.6, 1.5, 0.5 Hz), 9.27 (1H, s). δ (ppm) ¹³C, 400 MHz, CDCl₃) 127.1, 148.76202, 147.26062, 136.10001, 56.15704, 106.39285, 153.92217, 128.7, 113.86571, 162.19412, 103.05, 150.1025, 133.39999, 151.63397, 159.867, 149.17067, 120.3, 162.19412, 130, 130.55386, 56.15704. ESI-MS: 455.30. Anal. Calc. for C₂₁H₁₆Cl₂N₆O₂: C, 55.40; H, 3.54; Cl, 15.57

N, 18.46; O, 7.03. Found: C, 55.35; H, 3.51; Cl, 15.51 N, 18.42. HR-MS (ESI) *m/z*: Calculated for [M+H] ⁺455.302; found: 452.198

N4-(4-chlorobenzylidene)-N2-(4-chloropyrimidin-2-yl)-6,7-dimethoxyquinazolin-2,4-diamine (SM-3): White crystals, (Yield: 95 %), (M.P.: 250 °C); ¹H NMR (400 MHz, CDCl₃): δ 3.88 (3H, s), 3.95 (3H, s), 6.74 (1H, d, *J* = 5.7 Hz), 7.11 (1H, d, *J* = 0.4 Hz), 7.56 (1H, d, *J* = 0.4 Hz), 7.73 (2H, ddd, *J* = 8.4, 1.3, 0.5 Hz), 7.82 (1H, d, *J* = 5.7 Hz), 7.89 (2H, ddd, *J* = 8.4, 1.5, 0.5 Hz), 9.13 (1H, s). δ (ppm) ¹³C (400 MHz, CDCl₃) 106.39285, 162.19412, 56.15704, 162.19412, 113.86571, 147.26062, 103.05, 162.60001, 148.76202, 149.17067, 135.6863, 151.63397, 134.64209, 56.15704, 150.1025, 120.3, 153.92217, 129.45, 129.45, 129.26, 129.26. Anal. Calc. for C₂₁H₁₆Cl₂N₆O₂: C, 55.40; H, 3.54; Cl, 15.57 N, 18.46; O, 7.03. Found: C, 55.35; H, 3.51; Cl, 15.51 N, 18.42. HR-MS (ESI) *m/z*: Calculated for [M+H] ⁺455.302; found: 452.197

N2-(4-chloropyrimidin-2-yl)-N4-(2,4-dichlorobenzylidene)-6,7-dimethoxyquinazolin-2,4-diamine (SM-4): White crystals, (Yield: 90 %), (M.P.: 280 °C); ¹H NMR (400 MHz, CDCl₃): δ 3.90 (3H, s), 3.94 (3H, s), 6.74 (1H, d, *J* = 5.7 Hz), 7.09 (1H, d, *J* = 0.4 Hz), 7.30 (1H, dd, *J* = 1.7, 0.5 Hz), 7.37 (1H, dd, *J* = 8.2, 1.7 Hz), 7.53 (1H, d, *J* = 0.4 Hz), 7.82 (1H, d, *J* = 5.7 Hz), 8.30 (1H, dd, *J* = 8.2, 0.5 Hz), 9.25 (1H, s). δ (ppm) ¹³C (400 MHz, CDCl₃) 133.16007, 153.92217, 148.76202, 162.19412, 106.39285, 150.1025, 159.867, 135.26233, 151.63397, 56.15704, 56.15704, 147.26062, 113.86571, 120.3, 133.39999, 103.05, 162.19412, 149.17067, 129.15804, 127.82146, 128.50981. Anal. Calc. for C₂₁H₁₅Cl₃N₆O₂: C, 51.50; H, 3.09; Cl, 21.72; N, 17.16; O, 6.53. Found: C, 51.46; H, 3.01; N, 17.11; Cl, 21.70; O, 6.51. HR-MS (ESI) *m/z*: Calculated for [M+H] ⁺489.747; found: 481.254.

N2-(4-chloropyrimidin-2-yl)-N4-(2,3-dichlorobenzylidene)-6,7-dimethoxyquinazolin-2,4-diamine (SM-5): White crystals, (Yield: 92 %), (M.P.: 240 °C); ¹H NMR (400 MHz, CDCl₃): δ 3.87-3.89 (6H, 3.88 (s), 3.87 (s)), 6.74 (1H, d, *J* = 5.7 Hz), 7.10 (1H, d, *J* = 0.4 Hz), 7.41 (1H, dd, *J* = 7.7, 7.6 Hz), 7.57 (1H, d, *J* = 0.4 Hz), 7.80-7.85 (2H, 7.82 (d, *J* = 5.7 Hz), 7.82 (dd, *J* = 7.7, 1.5 Hz)), 7.94 (1H, dd, *J* = 7.6, 1.5 Hz), 9.31 (1H, s). δ (ppm) ¹³C (400 MHz, CDCl₃) 113.86571, 162.19412, 56.15704, 120.3, 151.63397, 149.17067, 130.87527, 133.69477, 106.39285, 132.6984, 150.1025, 147.26062, 159.867, 127.83631, 56.15704, 130, 153.92217, 103.05, 148.76202, 162.19412, 133.39999. Anal. Calc. for C₂₁H₁₅Cl₃N₆O₂: C, 51.50; H, 3.09; Cl, 21.72; N, 17.16; O, 6.53. Found: C, 51.46; H, 3.01; N, 17.11; Cl, 21.70; O, 6.51. HR-MS (ESI) *m/z*: Calculated for [M+H] ⁺489.747.

N2-(4-chloropyrimidin-2-yl)-N4-(4-fluorobenzylidene)-6,7-dimethoxyquinazolin-2,4-diamine (SM-6): White crystals, (Yield: 91 %), (M.P.: 260 °C); ¹H

NMR (400 MHz, CDCl₃): δ 3.88 (3H, s), 3.94 (3H, s), 6.74 (1H, d, *J* = 5.7 Hz), 7.08 (1H, d, *J* = 0.4 Hz), 7.52-7.58 (3H, 7.55 (ddd, *J* = 8.3, 1.1, 0.5 Hz), 7.55 (d, *J* = 0.4 Hz)), 7.82 (1H, d, *J* = 5.7 Hz), 7.96 (2H, ddd, *J* = 8.3, 1.5, 0.5 Hz), 9.12 (1H, s). δ (ppm) ¹³C (400 MHz, CDCl₃) 106.39285, 163.35171, 113.86571, 162.60001, 56.15704, 162.19412, 149.17067, 162.19412, 153.92217, 147.26062, 148.76202, 120.3 150.1025, 130.06667, 130.06667, 56.15704, 151.63397, 103.05, 134.64209, 115.73111, 115.73111. Anal. Calc. for C₂₁H₁₆ClFN₆O₂: C, 57.48; H, 3.67; Cl, 8.08; F, 4.33; N, 19.15; O, 7.29. Found: C, 57.44; H, 3.61; Cl, 8.01; F, 4.31; N, 6.92; O, 7.21. HR-MS (ESI) *m/z*: Calculated for [M+H]⁺438.848.

N2-(4-chloropyrimidin-2-yl)-N4-(2,6-dichlorobenzylidene)-6,7-dimethoxyquinazoline-2,4-diamine (SM-7) : White crystals, (Yield: 93 %), (M.P.: >270 °C); ¹H NMR (400 MHz, CDCl₃): δ 3.90 (3H, s), 3.94 (3H, s), 6.74 (1H, d, *J* = 5.7 Hz), 7.09 (1H, d, *J* = 0.4 Hz), 7.43 (2H, dd, *J* = 7.8, 1.4 Hz), 7.52-7.57 (2H, 7.55 (t, *J* = 7.8 Hz), 7.53 (d, *J* = 0.4 Hz)), 7.82 (1H, d, *J* = 5.7 Hz), 9.27 (1H, s). δ (ppm) ¹³C (400 MHz, CDCl₃) 148.76202, 106.39285, 129.25, 129.25, 120.3, 130.3, 113.86571, 103.05, 159.867, 150.1025, 162.19412, 56.15704, 56.15704, 153.92217, 147.26062, 162.19412, 149.17067, 135.2, 135.2, 151.63397, 132.7. Anal. Calc. for C₂₁H₁₅Cl₂N₆O₂: C, 51.50; H, 3.09; Cl, 21.72; N, 17.16; O, 6.53. Found: C, 51.46; H, 3.01; N, 17.11; Cl, 21.70; O, 6.51. HR-MS (ESI) *m/z*: Calculated for [M+H]⁺489.747.

4-(((2-((4-chloropyrimidin-2-yl)amino)-6,7-dimethoxyquinazolin-4-yl)imino)methyl) phenol (SM-8): White crystals, (Yield: 83 %), (M.P.: 260 °C); ¹H NMR (400 MHz, CDCl₃): δ 3.86 (3H, s), 3.90 (3H, s), 6.74 (1H, d, *J* = 5.7 Hz), 6.99 (2H, ddd, *J* = 8.1, 1.1, 0.4 Hz), 7.04 (1H, d, *J* = 0.4 Hz), 7.69 (1H, d, *J* = 0.4 Hz), 7.79-7.85 (3H, 7.82 (ddd, *J* = 8.1, 1.4, 0.4 Hz), 7.82 (d, *J* = 5.7 Hz)), 9.10 (1H, s). δ (ppm) ¹³C (400 MHz, CDCl₃) 56.15704, 148.76202, 56.15704, 106.39285, 120.3, 162.60001, 151.63397, 113.86571, 103.05, 149.17067, 150.1025, 134.64209, 162.19412, 147.26062, 157.82517, 128.74625, 128.74625, 153.92217, 115.0105, 115.0105, 162.19412. Anal. Calc. for C₂₁H₁₇ClN₆O₃: C, 57.74; H, 3.92; Cl, 8.12; N, 19.24; O, 10.99. Found: C, 57.71; H, 3.91; Cl, 8.10; N, 19.22; O, 10.98. HR-MS (ESI) *m/z*: Calculated for [M+H]⁺436.857; found: 436.168.

N2-(4-chloropyrimidin-2-yl)-N4-(furan-2-ylmethylidene)-6,7-dimethoxyquinazoline-2,4-diamine (SM-9): White crystals, (Yield: 88 %), (M.P.: 250 °C); ¹H NMR (400 MHz, CDCl₃): δ 3.86 (3H, s), 3.87 (3H, s), 6.54 (1H, dd, *J* = 3.5, 1.8 Hz), 6.70 (1H, d, *J* = 5.7 Hz), 6.89 (1H, d, *J* = 0.5 Hz), 7.16 (1H, dd, *J* = 3.5, 0.8 Hz), 7.67 (1H, d, *J* = 0.5 Hz), 7.81-7.85 (2H, 7.83 (d, *J* = 5.7 Hz), 7.83 (dd, *J* = 1.8, 0.8 Hz)), 8.78 (1H, s). δ (ppm) ¹³C (400 MHz, CDCl₃) 112.4, 56.15704, 151.63397, 143.5, 150.64, 150.1025, 143.25, 106.39285, 162.19412, 148.76202, 103.05, 147.26062, 56.15704,

120.3, 109.5, 153.92217, 149.17067, 162.19412, 113.86571. Anal. Calc. for C₁₉H₁₅ClN₆O₃: C, 55.55; H, 3.68; Cl, 8.63; N, 20.46; O, 11.68. Found: C, 55.54; H, 3.61; Cl, 8.61; N, 20.42; O, 11.66. HR-MS (ESI) *m/z*: Calculated for [M+H]⁺410.819.

N4-(2-chloro-6-fluorobenzylidene)-N2-(4-chloropyrimidin-2-yl)-6,7-dimethoxy quinazoline-2,4-diamine (SM-10): White crystals, (Yield: 79%), (M.P.: 270 °C); ¹H NMR (400 MHz, CDCl₃): δ 3.90 (3H, s), 3.93 (3H, s), 6.74 (1H, d, *J* = 5.7 Hz), 7.07 (1H, d, *J* = 0.4 Hz), 7.25 (1H, dd, *J* = 1.7, 0.5 Hz), 7.53 (1H, d, *J* = 0.4 Hz), 7.56 (1H, dd, *J* = 7.8, 1.7 Hz), 7.82 (1H, d, *J* = 5.7 Hz), 7.92 (1H, dd, *J* = 7.8, 0.5 Hz), 9.24 (1H, s). δ (ppm) ¹³C (400 MHz, CDCl₃) 113.86571, 106.39285, 164.55, 148.76202, 153.92217, 150.1025, 120.3, 56.15704, 56.15704, 159.867, 151.63397, 162.19412, 117.95, 115.16124, 103.05, 147.26062, 133.39999, 127.82146, 149.17067, 162.19412, 133.16007. Anal. Calc. for C₂₁H₁₅Cl₂FN₆O₅: C, 53.29; H, 3.19; Cl, 14.98; F, 4.01; N, 17.76; O, 6.76. Found: C, 53.24; H, 3.11; N, 17.72; Cl, 14.97; F, 4.00; O, 6.75. HR-MS (ESI) *m/z*: Calculated for [M+H]⁺473.29.

2. Biological Evaluation

2.1. In Vitro Anti-proliferative Activity

The HT-29 and COLO-205 colorectal cancer cell lines were chosen because the docking scores for VEGFR and c-MET were the highest, and overexpression of these two receptors is common in colorectal cancer. SRB tests were used to assess the anti-proliferative properties of the synthesised compounds against HT-29 and COLO-205 cells. Cells were injected into 96 well microtiter plates in 90 L at 5000 cells per well for the current screening experiment. Following cell inoculation, the microtiter plates were incubated for 24 hours at 37 °C, 5 % CO₂, 95 % air, and 100 % relative humidity before adding the experimental medicines. To prepare a stock of 10⁻² concentration, the experimental medicines were solubilized in a suitable solvent. Cells were fixed *in-situ* by the gentle addition of 50 μL of cold 30 % (w/v) TCA (final concentration, 10 % TCA) and incubated for 60 minutes at 4 °C, thereafter SRB assays were performed. The absorbance was read on an ELISA plate reader at a wavelength of 540 nm, with a reference wavelength of 690 nm.

2.2. Enzyme Inhibition Assay

In vitro inhibition kinase assays were carried out by Averin Biotech Pvt. Ltd, Hyderabad. The general procedure was as follows: Cells were cultured in a 6-well plate at a density of 0.5 x 10⁶ cells/2 ml and incubated in a CO₂ incubator overnight at 37 °C for 24 hours. After the incubation period, spent media was removed and IC₅₀ concentrations of compounds were added and the cell was incubated for 72 h. At the end of the treatment, the media from all the wells were

transferred into 12 x 75 mm polystyrene tubes and washed with 500 μ l PBS (the PBS were saved in the same tubes). The PBS was removed and 250 μ l of trypsin-EDTA solution was added before incubating at 37 °C for 3-4 minutes. The culture media was poured back into their respective wells and the cells were harvested directly into 12 x 75 mm polystyrene tubes. The tubes were centrifuged for five minutes at 300 x g at 25 °C. The supernatant was carefully decanted. The PBS was washed twice and decanted completely. The cells were stained with 20 μ l of VEGFR-2 and HGF conjugated with PE and incubated away from light at 37 °C for 30 min. Cells were gently resuspended in 400 μ l pre-warmed DPBS and analyzed by flow cytometry using the 496 nm laser for excitation and detection at 578 nm (FL2).

2.3. Cell Apoptosis Assay

HT-29 cells were seeded into 6-well plates (4×10^5 / well) and incubated for 24 h. The cells were treated with 10 μ M concentrations of the tested compound SM-8 for 24 h. The cells were then washed twice with PBS and stained with Hoechst 33258 working solution for 30 mins at 37 °C under 5% CO₂. The morphological changes of apoptotic cells were observed with a fluorescence microscope (Leica DMI 400B) with a blue filter.

2.4. Cell Cycle Analysis

HT-29 cancer cells treated by the most potent compound, SM-8, were analysed by flow cytometry analysis using a PI staining assay. The HT-29 cells were treated with IC₅₀ concentrations of the test compound for 24 h. For cell cycle analysis, Hoechst 33342 trihydrochloride trihydrate was used, which indicates the concentration of double stranded DNA in the cell. Then the cells were trypsinized, washed with PBS and centrifuged at 1000 rpm for 5 min. Novocyte flow cytometry (RGCB) was used to calculate the cell cycle distribution by NovoExpress 1.1.0 software.

3. Molecular Docking, *in-silico* Physicochemical Properties and ADME Prediction

Schrodinger Maestro 12.3 was used to do the molecular docking. The X-ray co-crystal structure of kinase was downloaded from the RCSB Protein Data Bank (Research Collaboratory for Structural Bioinformatics PDB) and constructed using the Protein Preparation Wizard, with constraints imposed and default settings utilised in the Schrodinger suite's Maestro graphical user interface. The compounds were exposed to Qikprop, Schrodinger 12.3 molecular properties prediction in order to analyse and predict both physicochemical and pharmacokinetic relevant properties to assess the overall quality of the developed derivatives as therapeutic candidates.

In order to calculate the ligand binding free energies of the complex system, the Prime plug-in was used. MM/MGSB (Molecular Mechanics, The Generalized Born Model and Solvent accessibility) was performed to calculate the ligand binding free energies and ligand strain energies for the docked lead compound with c-MET (PDB code: 3LQ8) and VEGFR (PDB code: 4ASD) (Table 4). Polar solvation energies, non-polar solvation energies, and potential energies are the three basic components of binding free energy. Prime MM-GBSA is a plug-in that incorporates the advanced OPLS-2005 force field, the SGB solvation model for polar solvation (GBSA), non-polar solvation (GNP) and molecular mechanics energies (EMM), as well as non-polar accessible surface area and Vander Waals interactions. When ligand binding occurs, the free energy changes and is determined using the following equation:

$$\Delta G_{\text{bind}} = G_{\text{complex}} - (G_{\text{protein}} + G_{\text{ligand}})$$
$$G = \text{EMM} + \text{GSCB} + \text{GNP}$$

Where

G complex = Complex energy

G protein = Receptor energy

G ligand = Unbound ligand energy

EMM = Molecular mechanics energies

GSCB = SCB solvation model for polar solvation

GNP = non-polar solvation term

RESULTS AND DISCUSSION

1. Chemistry

2-Chloro-6, 7, dimethoxyquinazolin-4-amine was subjected to reflux for 24 h with a substituted benzaldehyde using glacial acetic acid as a catalyst and ethanol as a solvent. The substituted benzylidene-2-chloro-6,7-dimethoxyquinazolin-4-amine was obtained as an intermediate and was reacted with 2-amino-5-chloropyrimidine using DMSO and three equivalents of K₂CO₃ under reflux for 24 h to afford the final product, a substituted benzylidene-(5-chloropyrimidin-2-yl)-6,7-dimethoxyquinazolin-2,4-diamine (Scheme 1).

2. Biological Evaluation

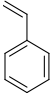
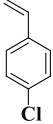
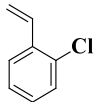
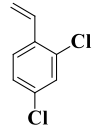
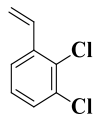
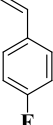
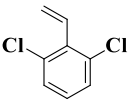
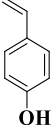
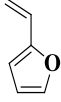
2.1. *In vitro* Anti-proliferative Activity

The designed synthesized target compounds were evaluated for their cytotoxicity against two cell lines viz. HT-29 and COLO-205 (human colorectal cancer; NCI, USA) by Sulforhodamine B (SRB) cell proliferation assays (the study was out-sourced at Tata

ACTREC). The results were expressed as GI_{50} i.e. concentration of drug causing 50 % inhibition of cell growth values and are summarized in **Table 1**. The cytotoxicity study clearly indicates that four target compounds showed good cytotoxicity against the HT-29 and COLO-205 cancer cell lines. Among them,

SM-2 (GI_{50} = 13.28 μ M), **SM-8** (GI_{50} = 12.42 μ M) and **SM-10** (GI_{50} = 19.44 μ M) showed good activity against COLO-205; whereas, **SM-8** (GI_{50} = 10.64 μ M), **SM-6** (GI_{50} = 33.64 μ M) and **SM-9** (GI_{50} = 18.81 μ M) showed good inhibition activity against HT-29 cell lines.

Table 1. Antiproliferative screening of the synthesized compounds on HT-29 and COLO-205 cell lines

Compounds	R	GI_{50} (μ M)	
		HT-29	COLO-205
SM-1		131.06	57.2
SM-2		136.61	13.28
SM-3		135.79	25.23
SM-4		124.60	20.38
SM-5		182.65	115.17
SM-6		33.64	112.75
SM-7		106.74	36.06
SM-8		10.64	12.42
SM-9		18.81	129.3

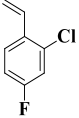
SM-10		182.94	19.44
Doxorubicin		<10	<10

Table 2. Table showing the % of inhibition of VEGFR-2 marker in untreated, standard and SM-8 treated COLO-205 and HT-29 cells

Test/ Marker	VEGFR-2 (% of inhibition)	
	COLO-205	HT-29
Cell Control	0.44	0.18
Doxorubicin	69.55	68.29
SM-8	65.31	66.11

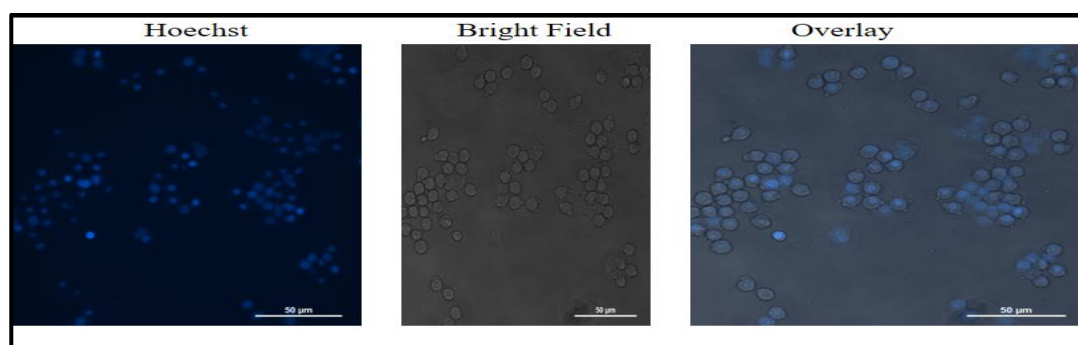


Figure. 2: Apoptotic assay by Hoechst 33258. HT-29 cells were treated with SM-8 (10µm) for 24 hrs and then stained with Hoechst 33258.

2.2. VEGFR-2 Inhibition Study

As VEGF pathway inhibition may trigger the upregulation of MET expression which may stimulate tumour invasion, a VEGFR-2 inhibition assay was performed. Moreover, the MET signalling pathway is considered a mechanism of resistance to vascular endothelial growth factor receptor therapy. The most active synthesized compound, **SM-8** was subjected to VEGFR-2 inhibitory activity. Doxorubicin was used as a positive control which showed inhibition values of 69.55 % (COLO-05) and 68.29 % (HT-29), whereas synthesized **SM-8** showed 65.31 % (COLO-205) and 66.11 % (HT-29) inhibition (**Table 2**).

2.3. Cell Apoptosis Assay

Hoechst 33258 staining was performed in order to investigate the nuclear morphological changes in **SM-8** on HT-29 cells. Hoechst 33258 is a fluorescent stain labelled DNA. In this, the live cell nuclei will be stained light blue and apoptotic cell nuclei will be stained dark

blue because of chromatin condensation. As shown in **Figure 2**, higher levels of apoptotic cells with nuclear condensation, nuclear fragmentation and enhanced brightness were detected following the treatment with 10 µM of molecule **SM-8**. From the above results, induction of cell apoptosis contributed to the anti-tumour effects of compound **SM-8**.

2.4. Cell Cycle Analysis

The inhibition of cancer cell proliferation at specific check-points was investigated by cell cycle analysis in HT-29 cancer cells. To further investigate the inhibitory pattern of compound **SM-8** at the IC₅₀ concentration for 24 h, the treated cells were harvested and stained with Hoechst 33342 trihydrochloride trihydrate stain and analysed by flow cytometry. Non-treated HT-29 cells were used as a control. As shown in **Figure 3**, at IC₅₀ concentration, the percentage of G1 phase cells increased from 75.8% in the control group to 77%. These results confirmed that compound **SM-8** significantly caused inhibition of HT-29 cancer cells.

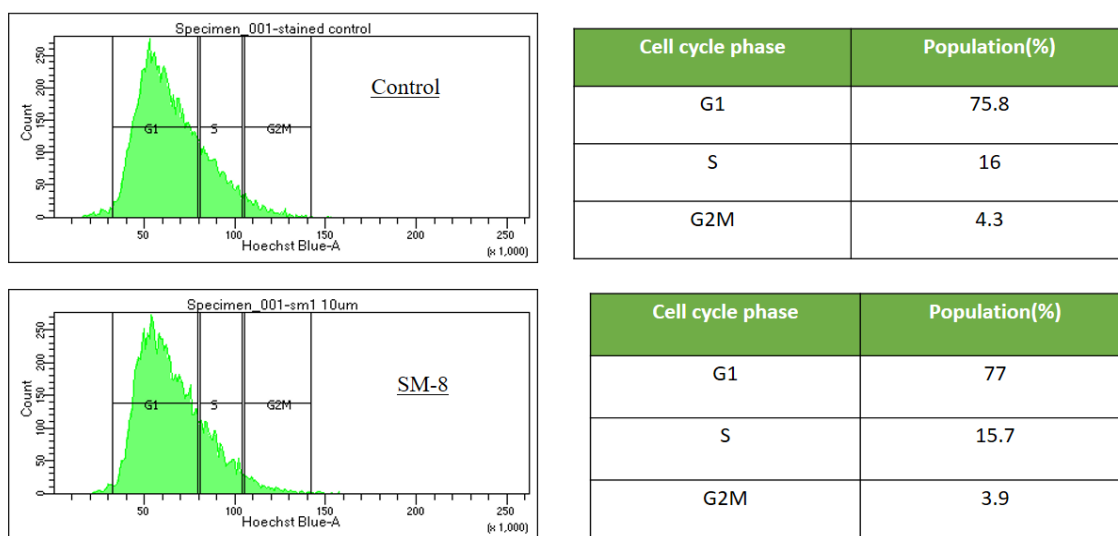


Figure 3. Cell cycle distribution of HT-29 cells treated with compound SM-8 and control

Table 3. Docking scores of the synthesized compounds against selected receptors with PDB IDs

Compound	VEGFR (PDB ID: 4ASD)	c-MET (PDB ID: 3LQ8)
SM-1	-8.807	-7.174
SM-2	-8.995	-6.793
SM-3	-9.035	-6.229
SM-4	-9.089	-6.551
SM-5	-8.766	-6.671
SM-6	-9.201	-6.940
SM-7	-7.770	-7.159
SM-8	-9.766	-6.790
SM-9	-8.605	-7.119
SM-10	-7.770	-6.921
Cabozantinib	-10.547	-8.473

3. *In-silico* Screening of Designed Derivatives

3.1. Molecular Docking

The significant inhibitory activity of the synthesized compounds was investigated through molecular docking inside the active site of the VEGFR-2 crystal structure (PDB: 4ASD) and c-MET (PDB: 3LQ8). Thus, in order to understand the interaction between the designed compounds and kinase, molecular docking was performed using Schrodinger Maestro 12.3 software. The docking study was carried out using cabozantinib as the standard drug in order to find better scores and interactions. The results are shown in **Table 3**.

As shown in **Figure 4**, the N of the pyrimidine ring and NH group of the imines were found to interact with **MET1160** while OH interacted with **TYR 1159** in the c-Met ATP binding site (PDB code: 3LQ8).

The docking study with VEGFR (PDB code: 4ASD) revealed that the pyrimidine and quinazolines rings interacted with **ILE 1023** and **ASP 1044**, whereas OH interacted with **ALA879**, which are all considered significant binding sites. The **SM-2, SM-3, SM-4, SM-6 and SM-8 (Figure 5)** had good docking results against both c-MET and VEGFR receptors. The above docking results proved that the compounds with good docking results may be used as candidates for anticancer drugs.

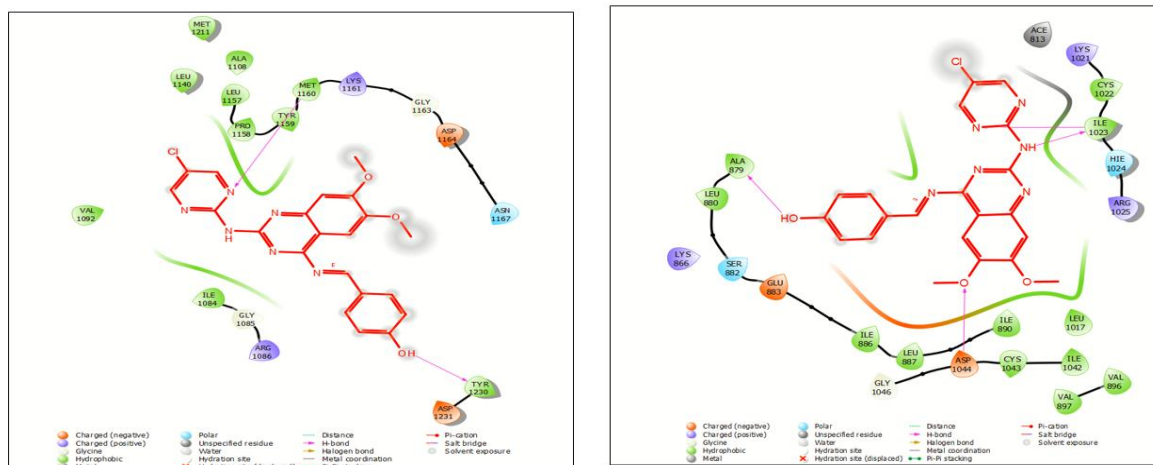


Figure 4. Molecular Docking and 2D Ligand interaction diagram of A) SM-8 c-MET: PDB code: 3LQ8 and B) SM-8 VEGFR: PDB Code: 4ASD.

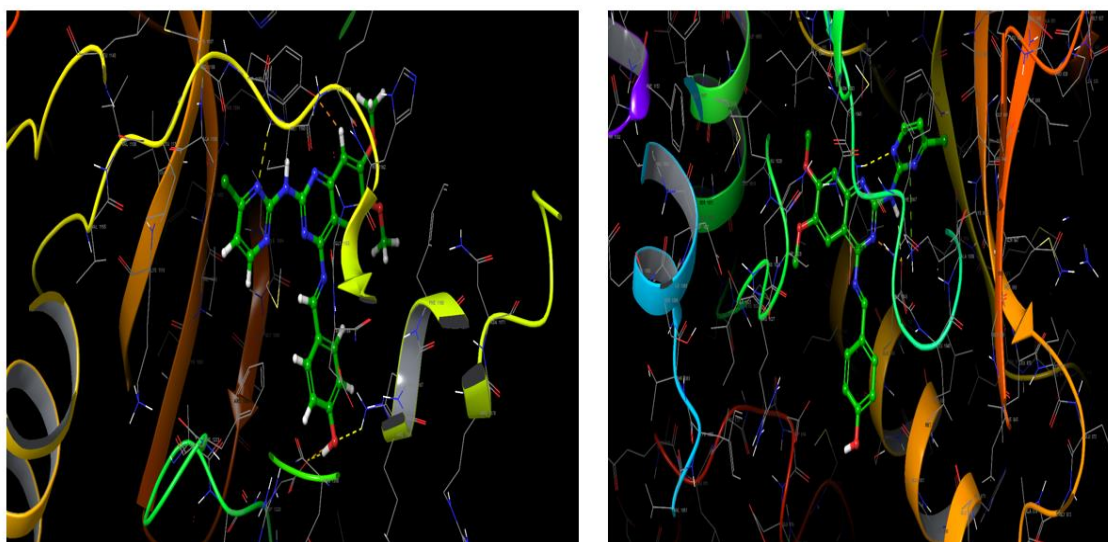


Figure 5. Molecular Docking and 3D visualization of SM-8 c-Met (PDB code: 3LQ8) and VEGFR (PDB Code: 4ASD).

Table 4. *In-silico* physicochemical properties of the most promising compounds

Compound	M.W	LogP	QPlogPo/w	n-OH	n-OH-NH	Lipinski's rule of five	TPSA	%ABS
SM-1	420.85	4.5	4.374	7.00	1	0	77.69	82.191
SM-2	455.30	5.2	4.867	7.00	1	1	77.70	82.194
SM-3	455.30	5.2	4.669	7.00	1	1	77.56	82.239
SM-4	489.74	5.8	5.1	7.00	1	1	77.53	82.249
SM-5	489.74	5.8	5.03	7.00	1	1	77.34	82.314
SM-6	438.84	4.7	4.61	7.00	1	1	77.71	82.188
SM-7	489.74	5.8	5.189	7.00	1	1	77.56	82.239
SM-8	436.85	4.2	3.669	7.500	2	0	100.27	74.406
SM-9	410.81	4.1	3.774	7.500	1	0	87.29	78.883
SM-10	473.29	5.3	4.843	7.00	1	1	77.57	82.238

Table 5. *In-silico* ADME prediction of the synthesized compounds

Compound	Number of metabolites	Predicted ADME		
		Human Oral Absorption (HOA %)	Blood Brain Barrier (BBB)	Plasma Protein binding (PPB %)
SM-1	3	86.831	-1	90.829
SM-2	3	100	0	90.829
SM-3	3	100	0	89.902
SM-4	3	100	0	89.139
SM-5	3	100	0	88.805
SM-6	3	100	0	92.073
SM-7	3	100	0	89.151
SM-8	4	100	-2	89.849
SM-9	4	100	0	85.713
SM-10	3	100	0	90.668

3.2. *In-silico* Physicochemical Properties and ADME Prediction

In-silico studies were performed to predict the physicochemical properties of the synthesized compounds. The important parameters were calculated by using Qikprop Schrodinger Maestro 12.3. % ABS was calculated by using the formula: $109 - (0.345 \times \text{TPSA})$ (Table 4).

The compounds under investigation showed log p values from 4.1 to 5.8 and were predicted to possess ranges from 1-2 for H-bond donors (n-OH/NH) and 7.0-7.5 for H-bond acceptors (n-ON). As for **QPlogPo/w**, the desired value was < 5. Among all the compounds, **SM-8** was found to have an acceptable value. In addition, these compounds had ABS values of 74.40 % to 82 %, indicating good oral bioavailability. Furthermore, compounds SM-1, SM-8 and SM-9 obeyed Lipinski's rule of five, suggesting that these compounds may be

used as lead structures for anticancer drugs. ADME properties were also calculated to evaluate overall drug quality. Results predicted that most active compounds had high human oral absorption values (86 % to 100 %), indicating well-absorbed compounds. CNS values were 0 to -2 and plasma protein binding values were 85.71 % to 92.07 % (Table 5).

3.3. Prime MM/GBSA Energies for Designed Compounds Complexed with c-MET (PDB: 3LQ8) and VEGFR-2 (PDB: 4ASD)

In order to calculate binding free energies, the most compatible plugin of Schrodinger was Prime MM/GBSA which included important factors such as hydrophobic, VDW, and solvation components. The screened compounds (**SM-1 to SM-10**) were subjected to MM/GBSA to calculate binding free energy. The calculated binding free energies of the designed docked compounds are shown in Table 6.

Table 6. The binding free energies of docked compounds using Prime MM/GBSA

No.	Complexed compounds	ΔG_{bind}^a (kcal/mol)	$\Delta G_{\text{coulomb}}^b$ (kcal/mol)	ΔG_{VDW}^c (kcal/mol)	$\Delta G_{\text{Solv. GB}}^d$ (kcal/mol)	Complex energy ^e (kcal/mol)
1.	SM-1-3LQ8	-154.416	91.705	76.694	94.726	-16450.08
2.	SM-2-3LQ8	-163.715	89.802	74.922	98.081	-16750.91
3.	SM-3-3LQ8	-168.326	76.656	77.262	75.503	-16440.12
4.	SM-4-3LQ8	-153.376	81.745	73.575	84.221	-15650.31
5.	SM-5-3LQ8	-169.218	85.336	73.925	86.321	-15750.05
6.	SM-6-3LQ8	-157.538	88.217	76.324	95.455	-15874.10
7.	SM-7-3LQ8	-168.920	94.702	71.471	91.928	-15806.54

8.	SM-8-3LQ8	-165.316	85.925	75.551	84.321	-15551.67
9.	SM-9-3LQ8	-154.870	89.426	73.624	89.451	-16340.87
10.	SM-10-3LQ8	-153.376	93.352	79.321	95.637	-16743.76
11.	SM-1-4ASD	-156.572	86.216	76.425	96.987	-15987.32
12.	SM-2-4ASD	-168.931	92.419	74.825	98.308	-15349.31
13.	SM-3-4ASD	-167.893	87.31	83.98	84.09	-16665.54
14.	SM-4-4ASD	-159.65	98.65	86.65	87.66	-15387.43
15.	SM-5-4ASD	-158.76	87.45	88.32	89.56	-17654.71
16.	SM-6-4ASD	-163.98	78.96	86.74	78.52	-16002.61
17.	SM-7-4ASD	-149.65	87.43	89.12	77.43	-15887.36
18.	SM-8-4ASD	-169.59	88.76	85.3	81.43	-16891.67
19.	SM-9-4ASD	-157.43	85.60	79.41	88.12	-14788.41
20.	SM-10-4ASD	-146.43	73.51	74.10	81.54	-14876.48

The binding energy is inversely proportional to the protein-ligand complex. The results indicated that **SM-2, SM-3, SM-4, SM-6 and SM-8** for c-MET (PDB: 3LQ8) and VEGFR-2 (PDB: 4ASD) had the most negative binding free energies, which confers binding stability. These MM/GBSA results suggest that the lead compounds satisfy the Prime MM/GBSA approach in order to achieve a stable complex with anticancer properties. Thus, all the energies predicted by the Prime MM/GBSA are thermodynamically favourable.

CONCLUSION

The novel derivatives of N-4-(substituted benzylidene)-N-2-(4-chloropyrimidin-2-yl)-6,7-dimethoxyquinazolin-2,4-diamine compounds were designed, synthesized and screened for their anticancer activity. *In-vitro* anti-proliferative activity against two human cancer cell-lines (HT-29 and COLO-205) activity was examined. The synthesized compounds **SM-2, SM-8 and SM-10** were found to be the most potent against COLO-205 and **SM-6, SM-8, and SM-9** against the HT-29 cell line. **SM-8** showed selectivity towards both cell lines. VEGFR-2 inhibitory activity studies of compound SM-8 showed 65.31 % (COLO-205) and 66.11 % (HT-29) against doxorubicin as standard. SM-8 blocked the proliferation of HT-29 cells at the G1 phase. In addition to the above findings, it is also important to determine the *in-vitro* and *in-vivo* mechanisms in depth. The docking study results showed that **SM-2, SM-3, SM-4, SM-6 and SM-8** showed good docking scores against both the selected proteins i.e., VEGFR (PDB code: 4ASD) and c-MET (PDB code: 4LQ8). Thus, the above results indicate that **SM-8** could serve as an important gateway for the design and development of new multi-target cancer cell inhibitors.

ACKNOWLEDGEMENTS

The authors are thankful to Mrs. Fatima Rafiq Zakaria, Chairman Maulana Azad Educational Trust, Dr. Rafiq Zakaria Campus, Aurangabad 431001(MS), India for providing the laboratory facilities. This work was supported by the Department of Science and Technology (DST), New Delhi, India [**Project File No. EEQ/2016/000055**]. The authors would like to extend their sincere appreciation to: Tata ACTREC for carrying out the anti-proliferative activity; Averin Biotech Pvt. Ltd, Hyderabad for the enzyme inhibition assay; Rajiv Gandhi Centre for Biotechnology for performing the cell cycle analysis and apoptosis assay; IIT SAIF, Mumbai for performing NMR and mass spectral analyses.

ORCID: Santosh N Mokale <https://orcid.org/0000-0002-9860-8895>.

Compliance with ethical standards

Conflict of interest:

The authors declare no conflict of interest, financial or otherwise.

Ethics approval and consent to participate:

This research did not require ethical approval as it did not involve any human or animal experimentation.

Human and animal rights:

No Animals/Humans were used for studies that are based on this research.

Consent for publication:

Not applicable.

Funding:

This research received no grant from any funding agency.

REFERENCES

1. Parang, K., Sun, G. (2005) Protein Kinase Inhibitors Drug Discovery. *Drug Discovery*.
2. Broekman, F., Giovannetti, E., Peters, G. J. (2011) Tyrosine kinase inhibitors: multi targeted or single- targeted. *J. Clin. Oncol.*, 80–93.
3. Folkman, J. (2002) Role of angiogenesis in tumor growth and metastasis. *Seminars in Oncology, Elsevier*, 15–18.
4. Wei, D., Fan, H., Zheng, K., Qin, X., Yang Y., Yang, L., Duan Y., Zhang Q., Zeng C., Hu L. (2019) Synthesis and anti-tumor activity of [2,3-f] quinazoline derivatives as dual inhibitors of c-MET and VEGFR-2. *Bioorg. Chem.*, **102916**.
5. Shi, W., Qiang, H., Huang, D., Bi, X., Huang, W., Qian, H. (2018) Exploration of novel pyrrolo [2,1-f] [1,2,4] triazine derivatives with improved anticancer efficacy as dual inhibitors of c-MET/ VEGFR-2. *E. J. Med. Chem.*, 814–831.
6. Ibrahmin, H., Awadallah, F., Refaat, H. M., Amin., K. M. (2018). Molecular docking simulation, synthesis and 3D pharmacophore studies of novel 2- substituted-5- nitro- benzimidazole derivatives as anticancer agents targeting c-MET and VEGFR-2. *Bioorg. Chem.*, 457–470.
7. Zhang, J., Jiang, X., Jian, Y., Guo, M., Zhang, S., Li, J., He, J., Liu, J., Wang, J., Ouyang, L. (2016) Recent advances in the development of dual VEGFR and c-MET small molecule inhibitors as anti-cancer drug. *Eur. J. Medchem.*, **108**, 495–504.
8. Lee, S. H., Jeong, D., Han, Y. S., Baek, M. J. (2015) Pivotal role of vascular endothelial growth factor pathway in tumor neovascularization. *Ann. Surg. Treat. Res.*, **89(1)**, 1–8.
9. Kitajima, Y., Ide, T., Ohtsuka, T., Miyazaki, K. (2008) Induction of hepatocyte growth factor activator gene expression under hypoxia activates the hepatocyte growth factor/ c-MET system via hypoxia inducible factor-1 in pancreatic cancer. *Cancer Sci.*, **99(7)**, 1341–1347.
10. Pennacchietti, S., Michieli, P., Galluzzo, M., Mazzone, M., Giordano, S., Comoglio, P. M. (2003) Hypoxia promotes invasive growth by transcriptional activation of the MET proto-oncogene. *Cancer Cell*, **3(4)**, 347–361.
11. Ramsay, R. R., Popovic-Nikolic, M. R., Nikolic, K., Uliassi, E., Bolognesi, M. L. (2018) A perspective on multi-target drug discovery and design for complex diseases. *Clin. Transl. Med.*, **7(1)**, 3.

List of Abbreviations

ADME: Absorption, Distribution, Metabolism and Excretion
MM/GBSA: Molecular Mechanics/ Generalized Born Surface Area
VEGFR: Vascular Endothelial Growth Factor
PDGF: Platelet- derived Growth Factor
FGF: Fibroblast Growth Factors
C-MET: Mesenchymal Epithelial Transition Factor
TLC: Thin Layer Chromatography
NMR: Nuclear Magnetic Resonance
DMF: Dimethylformamide
RCSB PDB: Research Collaboratory for Structural Bioinformatics PDB
EDTA: Ethylenediaminetetraacetic acid
DMSO: Dimethylsulphoxide
SRB: Sulforhodamine B